

Polarization dependence of emission spectra of multiexcitons in self-assembled quantum dots

N.Y. Hwang and S.-R. Eric Yang*

Physics Department, Korea University, Seoul Korea

We have investigated the polarization dependence of the emission spectra of p-shell multiexcitons of a quantum dot when the single particle level spacing is larger than the characteristic energy of the Coulomb interactions. We find that there are many degenerate multiexciton states. The emission intensities depend on the number of degenerate initial and final states of the optical transitions. However, unlike the transition energies, they are essentially independent of the strength of the Coulomb interactions. In the presence of electron-hole symmetry the independence is exact.

PACS numbers: 73.21.La, 78.66.-w, 71.45.Gm, 85.35.Be

I. INTRODUCTION

During recent years great progress has been made in the development of experimental tools for study of optical properties of single dot structures[1]: Confocal microscopy and near field scanning microscopy have been particularly useful. Self-assembled quantum dots(SAQDs) are promising as single photon generators[2, 3] because of the high optical quality of the resulting dot structures. Photons may be generated from states formed by a number of electrons and holes, i.e., multiexcitons[4, 5, 6, 7, 8, 9, 10, 11, 12, 13, 14, 15, 16, 17, 18, 19]. Fine structures of excitons, biexcitons, and triexcitons have been studied experimentally [4, 5, 6, 7, 8, 9, 10, 11]. Exact numerical diagonalization and quantum Monte Carlo studies of emission spectra of multiexciton states have been performed for several different shapes of SAQDs[12, 13, 14, 15, 16, 17, 18, 19]. The emission spectra of Bose-Einstein condensed magnetoexcitons in the strong magnetic field limit have been also investigated theoretically in SAQDs[20].

However, the polarization dependence of the emission spectra of multiexcitons in quantum dots is not well understood. In one-, two-, and three-dimensional electron-hole plasmas with parabolic bands the ratio between the emission intensities for linear and circular polarizations is constant since their optical strengths are M^2 and $2M^2$, see Table I. (The constant M is the dipole matrix element $-e\langle x|x|s\rangle$, where $|x\rangle$ and $|s\rangle$ are the Bloch wave functions). This is because the independent quasi-particle picture holds in these systems and each single particle state is always doubly spin degenerate. However, in zero-dimensional quantum dots this may not be the case since single particle levels are discrete and many body effects are strong, see Figs. 1 and 2. It is unclear to what extent the independent quasi-particle picture holds. A simple example demonstrates that there may be some polarization dependence. The emission from the s-shells is simple to analyse and shows that the emission spectra

for linear and circular polarizations are *not* proportional, see Fig. 2. This is because for $N = 2 \rightarrow 1$ and linear polarization the initial state of the optical transitions is non-degenerate while the final states are doubly *degenerate*. This means that the emission strength doubles from M^2 to $2M^2$. We investigate polarization dependence of the emission spectra of a quantum dot when a photon is generated by the recombination of an electron-hole pair in the p-shells, see Fig. 1. In this case the polarization dependence of the emission spectra is expected to be more complicated since many body states can be strongly correlated. Our results demonstrate that the optical strength can depend sensitively on the polarization state of the emitted photon. The optical strength can be enhanced significantly if there are several degenerate multiexciton final states. In addition the optical strength can take different values depending on which degenerate initial state of the optical transition is occupied. The emission spectra are calculated using these optical strengths, and are given in Figs. 3 and 4. The emission intensities are almost independent of the strength of the Coulomb interactions in our model, although the transition energies do depend on the Coulomb interactions. In the presence of electron-hole symmetry the independence is exact. Our results may be useful since they could provide an important qualitative result that must be valid in a more general approximation.

Polarization	$x + iy$	$x - iy$	x	y
$ e, 1/2\rangle \rightarrow h, -3/2\rangle$	0	$\sqrt{2}M$	M	iM
$ e, -1/2\rangle \rightarrow h, 3/2\rangle$	$\sqrt{2}M$	0	M	$-iM$

TABLE I: Transition matrix elements between a heavy hole and an electron for different polarizations. Note that a hole is the absence of a valence electron, and its spin takes the opposite value of the valence electron.

II. MODEL HAMILTONIAN

For our purpose we may take a simple model, which is illustrated in Fig. 1. In lens-shaped self-assembled quantum dots the conduction and valence band electrons can

*corresponding author, eyang@venus.korea.ac.kr

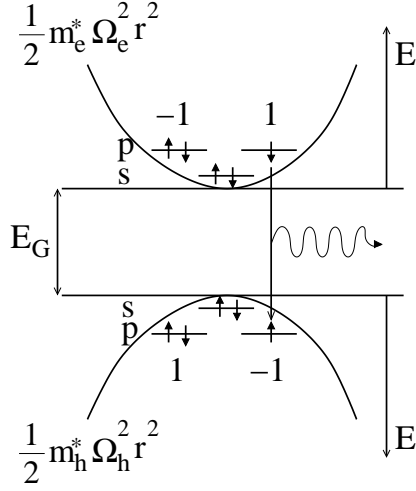


FIG. 1: Emission from the p-shells when N pairs of electrons and heavy holes occupy s- and p- orbitals of two-dimensional harmonic oscillators. Note that both electron and hole energies are measured positive. The bandgap E_G defined as the energy difference between the bottom of the electron harmonic potential and the top of the hole harmonic potential. The numbers 1 and -1 stand for the angular momentum components along the axis perpendicular to the two-dimensional layers.

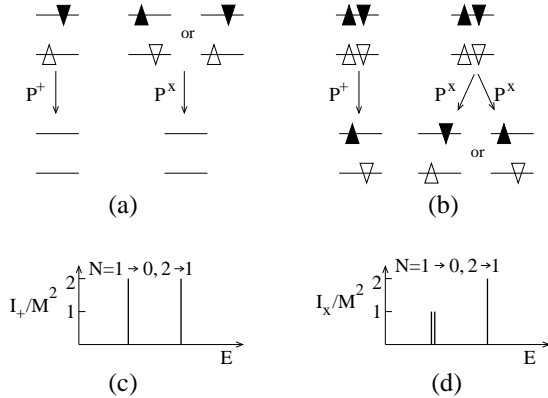


FIG. 2: Optical transitions between the s-shells. Filled (open) triangles represent electron (hole) spins. (a) Possible transitions for circular (P^+) and linear (P^x) polarizations when $N = 1 \rightarrow 0$. (b) Possible transitions when $N = 2 \rightarrow 1$. (c) Schematic display of the emission spectra for right circular polarization. (d) Emission spectra for linear polarization.

be approximated by those of harmonic oscillator wavefunctions. Since in quantum dots only states near $\vec{k} = 0$ are relevant we will neglect the heavy and light hole mixing and concentrate only on the physics of the heavy hole. The typical energy spacing between single particle energies is $20 - 40\text{meV}$, which is larger than the strength of the Coulomb interaction of order 10meV . The energies of s-level and p-level orbitals are denoted by $\epsilon_0^{e,h}$ and

$\epsilon_{\pm 1}^{e,h}$. Electron wavefunctions are $u_c(\vec{r})\chi(\pm\frac{1}{2})f_\ell(\vec{r})$ and heavy hole wavefunctions are $u_{v,\pm 1}(\vec{r})\chi(\pm\frac{1}{2})g_\ell(\vec{r})$. Here the conduction and heavy hole valence band Bloch wavefunctions are denoted by $u_c(\vec{r})$ and $u_{v,\pm 1}(\vec{r})$. In the following we will represent hole states $u_{v,1}(\vec{r})\chi(\frac{1}{2})g_\ell(\vec{r})$ and $u_{v,-1}(\vec{r})\chi(-\frac{1}{2})g_\ell(\vec{r})$ as having spin components $1/2$ and $-1/2$. The two-dimensional electron and hole effective mass wavefunctions are $f_\ell(\vec{r}_1)$ and $g_\ell(\vec{r}_2)$. The quantities $a_e^2 = \frac{\hbar}{2m_e^*\Omega_e}$ and $a_h^2 = \frac{\hbar}{2m_h^*\Omega_h}$ are the characteristic length scales for electrons and holes. The parameters m_e^* and m_h^* are the effective masses of electrons and holes, and Ω_e and Ω_h are the strengths of the harmonic potentials. Two-dimensional polar coordinates are r_1, r_2 and θ . We assume that the wavefunctions have a width d along the axis perpendicular to the two-dimensional plane. This effect is included in the shape of the Coulomb interactions. The *quasi-two-dimensional* Coulomb interaction has the form $V(\vec{r}_1, \vec{r}_2) = \frac{e^2}{\epsilon\sqrt{|\vec{r}_1 - \vec{r}_2|^2 + d^2}}$, where d is the width of the single particle wavefunctions along the z-axis (ϵ is the background dielectric constant). Single particle energies of electrons and holes are $\epsilon_\ell^e = \hbar\Omega_e(|\ell| + 1)$ and $\epsilon_\ell^h = \hbar\Omega_h(|\ell| + 1)$. Note the hole energy is defined to be positive. The bandgap E_G , defined as the energy difference between the bottom of the electron harmonic potential and the top of the hole harmonic potential, is set to zero. In our model we assume that the single particle level spacing is larger than or comparable to the characteristic Coulomb energy, which is often valid in lens-shaped SAQDs[21]. This allows us to ignore excitations from s to p levels and from p to d levels/continuum states of two-dimensional layers [21, 22]. We can thus assume that the s-shell is completely filled and inert.

The many body Hamiltonian H for the electron-hole system can be written as a sum of single particle terms H_0 and interaction terms V_{int} , i.e., $H = H_0 + V_{\text{int}}$ with $H_0 = H_e + H_h$ and $V_{\text{int}} = H_{ee} + H_{hh} + H_{eh}$, where the single particle Hamiltonians $H_e = \sum_{\ell,\sigma} \epsilon_\ell^e a_{\ell\sigma}^\dagger a_{\ell\sigma}$ and $H_h = \sum_{\ell,\sigma} \epsilon_\ell^h b_{\ell\sigma}^\dagger b_{\ell\sigma}$. The operator $a_{\ell,\sigma}^\dagger$ and $b_{\ell,\sigma}^\dagger$ create an electron and a heavy hole ($\sigma = \uparrow$ or \downarrow). Electron-electron, hole-hole, and electron-hole interaction terms are H_{ee} , H_{hh} , and H_{eh} , respectively. The electron Coulomb matrix elements are $U_{\alpha_1\alpha_2\alpha_4\alpha_3}^{ee} = \delta_{\sigma_1,\sigma_4}\delta_{\sigma_2,\sigma_3}\delta_{\ell_1+\ell_2,\ell_3+\ell_4}\langle f_{\ell_1}f_{\ell_2}|V|f_{\ell_4}f_{\ell_3}\rangle$ and hole Coulomb matrix elements are $U_{\beta_1\beta_2\beta_4\beta_3}^{hh} = \delta_{\sigma_1,\sigma_4}\delta_{\sigma_2,\sigma_3}\delta_{\ell_1+\ell_2,\ell_3+\ell_4}\langle g_{\ell_1}g_{\ell_2}|V|g_{\ell_4}g_{\ell_3}\rangle$ (α and β stand for (ℓ, σ)). The electron-hole matrix elements are $U_{\beta_1\alpha_2\beta_4\alpha_3}^{eh} = -\delta_{\sigma_1,\sigma_4}\delta_{\sigma_2,\sigma_3}\delta_{\ell_1+\ell_2,\ell_3+\ell_4}\langle g_{\ell_1}f_{\ell_2}|V|g_{\ell_4}f_{\ell_3}\rangle$. Since the single particle energies are independent of spin we can write $\epsilon_{\ell,\sigma}^e = \epsilon_\ell^e$. When $\delta_{\sigma_1,\sigma_4} = \delta_{\sigma_2,\sigma_3} = 1$ we may write $U_{\ell_1\sigma_1,\ell_2\sigma_2,\ell_4\sigma_4,\ell_3\sigma_3}^{ee} = V_{\ell_1,\ell_2,\ell_4,\ell_3}^{ee}$. Similarly, simpler notations may be introduced for U^{hh} and U^{eh} .

III. MULTIEXCITON HAMILTONIAN MATRIX

The total z-component of angular momentum $L_z = L_{e,z} + L_{h,z}$ is conserved. The electron and hole angular momenta, $L_{e,z}$ and $L_{h,z}$, need not be conserved separately since H_{eh} can change them. On the other hand the total z-component of spin for electrons (holes), $S_{e,z}$ ($S_{h,z}$), is conserved since H_{eh} cannot change $S_{e,z}$ or $S_{h,z}$. If $S_{e,z}$ is known then the electron spin quantum number S_e can be deduced: When $S_{e,z} = -1, 0$, or 1 then $S_e = 1$, and when $S_{e,z} = -\frac{1}{2}$ or $\frac{1}{2}$ then $S_e = \frac{1}{2}$. In our model $S_{e,z}$ cannot take other values than the ones just listed, see Fig. 5. Similar results hold for hole spins. We label the Hilbert subspaces by $|L_z, S_{e,z}, S_{h,z}\rangle$. The resulting Hilbert subspaces are listed in the Fig. 5 (see Appendix B).

The basis vectors in each Hilbert subspace may be chosen as the single Slater determinant states $|\phi_i\rangle = a_{\alpha_N}^\dagger \cdots a_{\alpha_1}^\dagger b_{\beta_N}^\dagger \cdots b_{\beta_1}^\dagger |0\rangle$, with $i = (\vec{\alpha}_i, \vec{\beta}_i)$ where $\vec{\alpha}_i = (\alpha_1, \alpha_2, \dots, \alpha_N)$ and $\vec{\beta}_i = (\beta_1, \beta_2, \dots, \beta_N)$. The k th eigenstate of N electron-hole system is written as $|\Phi_k\rangle = \sum_i A_i^k |\phi_i\rangle$. The eigenstate $|\Phi_k\rangle$ and eigenvalue E_k satisfy the following matrix equation $\sum_j \langle \phi_i | H | \phi_j \rangle A_j^k = E_k A_i^k$. The diagonal elements of the Hamiltonian matrix are

$$\langle \phi_i | H | \phi_i \rangle = E_e + E_h + E_{eh}. \quad (1)$$

The total energy of the electrons/holes can be determined from

$$E_p[n_\alpha] = \sum_\alpha \varepsilon_\alpha^p n_\alpha^p + \frac{1}{2} \sum_{\alpha\beta} n_\alpha^p n_\beta^p U_{\alpha\beta}^p, \quad (2)$$

with $U_{\alpha\beta}^p = U_{\alpha\beta\alpha\beta}^{pp} - U_{\alpha\beta\beta\alpha}^{pp}$, where $p = e, h$. The electron and hole occupation numbers in $|\phi_i\rangle$ are denoted by n_α^e and n_α^h . The total electron-hole interaction energy is $E_{eh} = \sum_{\alpha\beta} n_\alpha^e n_\beta^h U_{\alpha\beta}^{eh}$. The off-diagonal elements are

$$\langle \phi_i | H | \phi_j \rangle = \langle \phi_i | H_{ee} | \phi_j \rangle + \langle \phi_i | H_{hh} | \phi_j \rangle + \langle \phi_i | H_{eh} | \phi_j \rangle. \quad (3)$$

IV. EIGENSTATES

In our model it is possible to find analytically all the eigenstates in each Hilbert subspace. This is because the maximum number of basis states of these Hilbert subspaces is at the most six and the Hamiltonian matrices have simple forms.

A. Uncorrelated single Slater determinant states and correlated states with two basis vectors

In our model many Hilbert subspaces are one-dimensional. They are displayed in Fig. 5 and their

energies are given by Eq. (1). There are many two-dimensional Hilbert subspaces. Their Hamiltonian matrices are symmetric and the diagonal elements are the same:

$$\begin{pmatrix} \langle \phi_1 | H | \phi_1 \rangle & \langle \phi_1 | H | \phi_2 \rangle \\ \langle \phi_2 | H | \phi_1 \rangle & \langle \phi_2 | H | \phi_2 \rangle \end{pmatrix} = \begin{pmatrix} \gamma & \delta \\ \delta & \gamma \end{pmatrix}. \quad (4)$$

The eigenvalues of this matrix are

$$E_1 = \gamma + \delta, \quad E_2 = \gamma - \delta, \quad (5)$$

and the corresponding eigenvectors are

$$|\Phi_1\rangle = \frac{1}{\sqrt{2}}(|\phi_1\rangle + |\phi_2\rangle), \quad |\Phi_2\rangle = \frac{1}{\sqrt{2}}(|\phi_1\rangle - |\phi_2\rangle). \quad (6)$$

Note that these eigenvectors are *independent* of the Coulomb interactions. The off-diagonal element $\delta = \langle \phi_1 | H | \phi_2 \rangle$ is non-zero for $N = 3, 4, 5$.

B. Correlated states with six basis vectors

In our model there is only one Hilbert subspace with six basis states: the Hilbert subspace $|L_z, S_{e,z}, S_{h,z}\rangle = |0, 0, 0\rangle$ for $N = 4$. The basis vectors are defined as follows: $|\phi_1\rangle = a_{1,\uparrow}^\dagger a_{-1,\downarrow}^\dagger b_{1,\uparrow}^\dagger b_{-1,\downarrow}^\dagger |S\rangle$, $|\phi_2\rangle = a_{1,\uparrow}^\dagger a_{-1,\downarrow}^\dagger b_{1,\downarrow}^\dagger b_{-1,\uparrow}^\dagger |S\rangle$, $|\phi_3\rangle = a_{1,\downarrow}^\dagger a_{-1,\uparrow}^\dagger b_{1,\uparrow}^\dagger b_{-1,\downarrow}^\dagger |S\rangle$, $|\phi_4\rangle = a_{1,\downarrow}^\dagger a_{-1,\uparrow}^\dagger b_{1,\downarrow}^\dagger b_{-1,\uparrow}^\dagger |S\rangle$, $|\phi_5\rangle = a_{-1,\downarrow}^\dagger a_{1,\uparrow}^\dagger b_{1,\uparrow}^\dagger b_{-1,\downarrow}^\dagger |S\rangle$, $|\phi_6\rangle = a_{-1,\downarrow}^\dagger a_{1,\uparrow}^\dagger b_{1,\downarrow}^\dagger b_{-1,\uparrow}^\dagger |S\rangle$, where $|S\rangle = a_{0,\downarrow}^\dagger a_{0,\uparrow}^\dagger b_{0,\downarrow}^\dagger b_{0,\uparrow}^\dagger |0\rangle$ represents the filled s-shells. Note that $|\phi_5\rangle$ and $|\phi_6\rangle$ contain doubly occupied p-orbitals. The diagonal matrix elements are $A = \langle \phi_k | H | \phi_k \rangle$ and are given by Eq. (1). If we define $B = -V_{-1,1,1,-1}^{ee}$, $C = -V_{-1,1,1,-1}^{hh}$ and $D = V_{-1,1,1,-1}^{eh}$, the Hamiltonian matrix is given by

$$H = \begin{pmatrix} A & C & B & 0 & D & D \\ C & A & 0 & B & -D & -D \\ B & 0 & A & C & -D & -D \\ 0 & B & C & A & D & D \\ D & -D & -D & D & A & 0 \\ D & -D & -D & D & 0 & A \end{pmatrix}, \quad (7)$$

with the eigenvalues $E_1 = A + B + C$, $E_2 = \frac{1}{2}(2A - B - C - \sqrt{B^2 + 2BC + C^2 + 32D^2})$, $E_3 = A + B - C$, $E_4 = A$, $E_5 = A - B + C$ and $E_6 = \frac{1}{2}(2A - B - C + \sqrt{B^2 + 2BC + C^2 + 32D^2})$. The eigenvectors are

$$\begin{aligned} |\Phi_1\rangle &= \frac{1}{2}(|\phi_1\rangle + |\phi_2\rangle + |\phi_3\rangle + |\phi_4\rangle), \\ |\Phi_2\rangle &= a_1|\phi_1\rangle + a_2|\phi_2\rangle + a_3|\phi_3\rangle + a_4|\phi_4\rangle + a_5|\phi_5\rangle + a_6|\phi_6\rangle, \\ |\Phi_3\rangle &= \frac{1}{2}(-|\phi_1\rangle + |\phi_2\rangle - |\phi_3\rangle + |\phi_4\rangle), \\ |\Phi_4\rangle &= \frac{1}{\sqrt{2}}(-|\phi_5\rangle + |\phi_6\rangle), \\ |\Phi_5\rangle &= \frac{1}{2}(-|\phi_1\rangle - |\phi_2\rangle + |\phi_3\rangle + |\phi_4\rangle), \\ |\Phi_6\rangle &= b_1|\phi_1\rangle + b_2|\phi_2\rangle + b_3|\phi_3\rangle + b_4|\phi_4\rangle + b_5|\phi_5\rangle + b_6|\phi_6\rangle. \end{aligned} \quad (8)$$

Note again that $|\Phi_1\rangle, |\Phi_3\rangle, |\Phi_4\rangle$, and $|\Phi_5\rangle$ are *independent* of the Coulomb interactions and model parameters. On the other hand, the expansion coefficients of $|\Phi_2\rangle$ and $|\Phi_6\rangle$ do depend on them. The expansion coefficients can be obtained analytically but their expressions are rather complicated and lengthy. The lowest energy state is $|\Phi_1\rangle$ since $B < 0, C < 0$. In this state both electrons and holes are in a spin triplet state $S_e = 1$ and $S_h = 1$ with $(S_{e,z}, S_{h,z}) = (0, 0)$.

C. Number of groundstate degeneracy

Our investigation shows groundstates have $L_z = 0$, see Fig. 5. When $N = 6, 5, 4, 3, 2$ we see from Fig. 5 that the number of degenerate states with $L_z = 0$ are 1, 4, 9, 4, 1. Let us examine why the degeneracy is 9 for $N = 4$. From symmetry considerations one can predict the number of groundstate degeneracy. Confirming this number of degeneracy provides a powerful *check* of the correctness of our analytic calculation of eigenenergies. We find that the lowest energy states are the ones with electrons and holes in triplet states. The electron and hole spin numbers are thus $S_e = 1$ and $S_h = 1$. This implies that the possible values of $(S_{e,z}, S_{h,z})$ are $3 \times 3 = 9$. Since the interactions are spin invariant these states are degenerate. Our calculation shows that the groundstates of the following nine Hilbert subspaces $|0, 1, 1\rangle, |0, 0, 1\rangle, |0, 0, -1\rangle, |0, -1, -1\rangle, |0, -1, 1\rangle, |0, 1, -1\rangle, |0, -1, 0\rangle, |0, 1, 0\rangle$, and $|0, 0, 0\rangle$ are degenerate (see Fig. 5). Other degeneracies may be shown in a similar manner.

V. OPTICAL STRENGTH AND EMISSION SPECTRA

Transition types	Linear pol.	Circular pol.
Between single and two-basis states	$2M^2$	$4M^2$
Between two-basis states	M^2	$2M^2$
Between two- and six-basis states	$\frac{1}{2}M^2$	M^2

TABLE II: In our model most optical dipole strengths can take only four different values, $\frac{1}{2}M^2, M^2, 2M^2$ and $4M^2$. The oscillator strengths of circular polarization are twice those of linear polarization, just like in the case of single particle transitions.

In this paper we consider linearly, right circularly, and left circularly polarized photons. We assume fast energy relaxation so that only emission from ground states of N exciton pairs are needed. The emission spectrum is given by

$$I(\omega) = \sum_f |\langle \Phi_f | \hat{L} | \Phi_G \rangle|^2 \delta(E_i - E_f - \omega), \quad (9)$$

where the luminescence operator is

$$\hat{L} = \sum_{\ell, \sigma} \langle -\ell, -\sigma | \hat{\varepsilon} \cdot \vec{p} | \ell, \sigma \rangle b_{-\ell, -\sigma} a_{\ell, \sigma}. \quad (10)$$

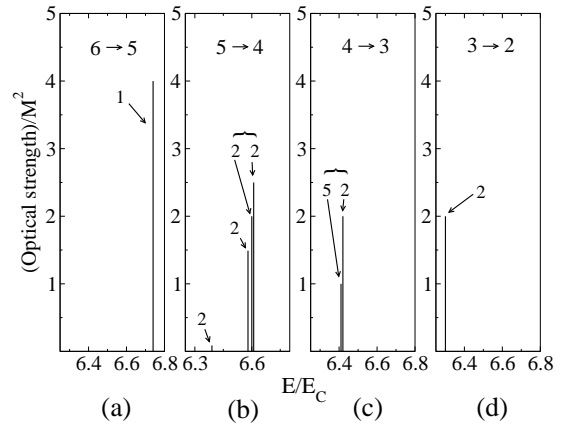


FIG. 3: Emission spectra for linear polarization P^x . Closely spaced vertical lines under the curly bracket have all the *same* transition energy. The numbers above the arrows denote the number of different initial states giving rise to the same transition energy. The change in the number of electron-hole pairs $N \rightarrow N - 1$ is indicated in the upper part of each panel.

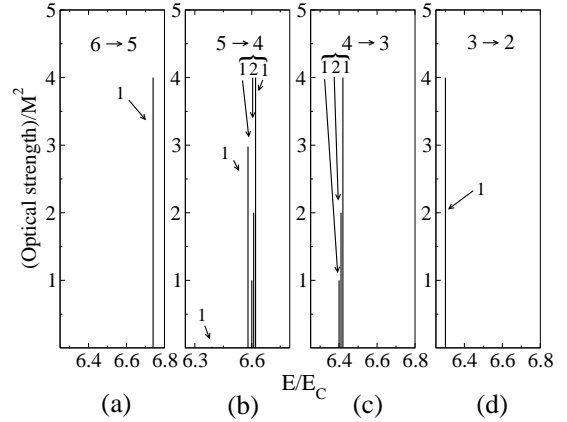


FIG. 4: Emission spectra for circular polarization P^+ .

An electron and a hole can only recombine when they have opposite values of the z-component of angular momenta and spins. This leads to the *selection rules* $\Delta L_z = 0$ and $\Delta S_z = 0$. The optical dipole strength from a ground state of N -exciton system, $\Phi_G(N)$, to a ground/excited state of $(N-1)$ -exciton system, $\Phi_f(N-1)$, is $|\langle \Phi_f | \hat{L} | \Phi_G \rangle|^2$. The possible values of the optical dipole strength are displayed in Table II. In our model there are only three types of dipole transitions: (a) transitions between single and two-basis states, (b) transitions between two-basis states, and (c) transitions between two- and six-basis states. We have computed emission spectra for polarization along the x-axis (P^x), left circular polarization (P^-), and right circular polarization (P^+). They are shown in Figs. 3 and 4. The following parameters are used: $a_h = 0.46a_e$, $d = 0.8a_e$, $\hbar\Omega_e = 2E_C$, and $\Omega_h = 0.7\Omega_e$. In our calculation we measure energy with

respect to the Coulomb energy $E_C = \frac{e^2}{\epsilon a_e}$. Note that the transition energy is actually $E_i - E_f + E_G$, but we will drop the bandgap energy E_G for convenience hereafter. The emission spectra for right and left circular polarizations are identical. Note that only one transition energy is possible when $N = 6 \rightarrow 5$, $4 \rightarrow 3$, and $3 \rightarrow 2$. This is because transitions from the ground state of $N = 6$ to the excited states of $N = 5$, and from the ground state of $N = 4$ to the excited states of $N = 3$ are optically forbidden or vanish. On the other hand, for $N = 5 \rightarrow 4$ three transition energies are possible. One can show that the excited states $|\Phi_3\rangle$, $|\Phi_4\rangle$ and $|\Phi_5\rangle$ of the Hilbert subspace $|0, 0, 0\rangle$ for $N = 4$ do not contribute to optical strengths (see Appendix A). Only $|\Phi_1\rangle$, $|\Phi_2\rangle$ and $|\Phi_6\rangle$ contribute.

Let us discuss the emission spectra of $5 \rightarrow 4$ for P^x . The oscillator strength of the lowest energy peak $6.39E_C$ is $0.0088M^2$. It originates from the transitions $|0, \frac{1}{2}, -\frac{1}{2}\rangle_1$ or $|0, -\frac{1}{2}, \frac{1}{2}\rangle_1 \rightarrow |\Phi_6\rangle$, see Fig. 5 (These are defined as type A transitions). The *subscript* 1 in $|0, \frac{1}{2}, -\frac{1}{2}\rangle_1$ indicates that it is the lowest energy eigenstate. This oscillator strength is negligible compared to those of the others. The oscillator strength of the next lowest transition energy $6.58E_C$ is $1.4912M^2$. It originates from the transitions $|0, \frac{1}{2}, -\frac{1}{2}\rangle_1$ or $|0, -\frac{1}{2}, \frac{1}{2}\rangle_1 \rightarrow |\Phi_2\rangle$ (These are defined as type B transitions). The dependence of the strength of this peak on the ratio Ω_h/Ω_e is negligible: as it is reduced from 0.7 to 0.1 the oscillator strength changes smoothly from $1.4912M^2$ to $1.5000M^2$ (the change is only about 1%). The dependence on the Coulomb interactions, i.e., on the ratio d/a_e is also negligible: as it is reduced from 0.8 to 0.2 the oscillator strength reduces continuously from $1.4912M^2$ to $1.4780M^2$. As these parameters change the sum of the two oscillator strengths of transitions A and B remains a constant equal to $3/2M^2$. This is *evidence* that our calculations are correct. The highest peak with the energy $6.61E_C$ has the optical strength $5/2M^2$ and originates from the transitions $|0, \frac{1}{2}, -\frac{1}{2}\rangle_1 \rightarrow |0, 1, -1\rangle_1$ and $|\Phi_1\rangle$, or $|0, -\frac{1}{2}, \frac{1}{2}\rangle_1 \rightarrow |0, -1, 1\rangle_1$ and $|\Phi_1\rangle$, see Fig. 5. In these transitions there are two possible final states with the same energy, and the oscillator strength is the sum of the two contributions. The other peak at the same transition energy with the strength $2M^2$ originates from the transitions $|0, \frac{1}{2}, \frac{1}{2}\rangle_1 \rightarrow |0, 1, 0\rangle_1$ and $|0, 0, 1\rangle_1$, or $|0, -\frac{1}{2}, -\frac{1}{2}\rangle_1 \rightarrow |0, -1, 0\rangle_1$ and $|0, 0, -1\rangle_1$. Note that some transition energies can have more than one optical strengths. For example, for $N = 5 \rightarrow 4$ at the transition energy $6.61E_C$ two values of optical strengths $2M^2$ and $5/2M^2$ are possible. In this case there are two different initial states giving rise to the same value of the optical strength $2M^2$. The same is also true for $5/2M^2$, see Fig. 3.

Now we discuss the emission spectra for P^+ for the case $N = 5 \rightarrow 4$. The oscillator strength of the lowest energy peak $6.39E_C$ is $0.0176M^2$. It originates from the transition $|0, -\frac{1}{2}, \frac{1}{2}\rangle_1 \rightarrow |\Phi_6\rangle$, see Fig. 5 (We define it as type C transition). This oscillator strength is negligible compared to those of the others. The oscillator strength

of the next lowest energy peak $6.58E_C$ is $2.9824M^2$. It originates from the transitions $|0, -\frac{1}{2}, \frac{1}{2}\rangle_1 \rightarrow |\Phi_2\rangle$ (We define it as type D transition). Again as the physical parameters change the sum of the two oscillator strengths of transitions C and D remains a constant equal to $3M^2$. Note that some transition energies can have more than one optical strengths. For example, for $N = 5 \rightarrow 4$ at the transition energy $6.61E_C$ three values of optical strengths M^2 , $2M^2$ and $4M^2$ are possible. The highest peak $6.61E_C$ with the strength $4M^2$ originates from the transitions $|0, \frac{1}{2}, -\frac{1}{2}\rangle_1 \rightarrow |0, 1, -1\rangle_1$. The peak $6.61E_C$ with the strength $2M^2$ originates from the transitions $|0, \frac{1}{2}, \frac{1}{2}\rangle_1 \rightarrow |0, 1, 0\rangle_1$, or $|0, -\frac{1}{2}, -\frac{1}{2}\rangle_1 \rightarrow |0, 0, -1\rangle_1$. The peak $6.61E_C$ with the strength M^2 originates from the transitions $|0, -\frac{1}{2}, \frac{1}{2}\rangle_1 \rightarrow |\Phi_1\rangle$. There are thus two different initial states giving rise to the same value of the optical strength $2M^2$, and there are only one initial states giving rise to the optical strengths M^2 and $4M^2$.

We have verified numerically that when electrons and holes have exactly the same properties, i.e., when *electron-hole symmetry* is present, the dependence of the oscillator strengths for the transitions A, B, C and D on the Coulomb interactions disappears completely. The oscillator strengths of these transitions become, respectively, 0 , $\frac{3}{2}$, 0 , and 3 .

VI. DISCUSSIONS

Our main results may be attributed to the presence of degenerate states and the strongly correlated nature of multiexciton states. In the non-interacting model, spin properties of electronic states do not change as a function of energy. In the interacting case, spin properties of electronic states do change as a function of energy. At different transition energies spin properties of optically active initial and final states are different. Which initial and final states are connected by the optical selection rules will depend on the polarization of the emitted photon. Several factors contribute to the quantitative aspects of the polarization dependence of the emission spectra. As illustrated in Fig. 2 the presence of degenerate final states can enhance the oscillator strengths. The presence of degenerate initial states can lead to the presence of degenerate transition energies. The correlated nature of some eigenstates influence the value of their oscillator strengths and can lead to a cancellation of the optical strength.

Our approximate calculation shows that there is a significant polarization dependence. For more realistic SAQDs our results may be used as a starting point of a perturbative treatment of the electron-hole exchange interaction, the coupling between s and p and between p and d levels, coupling between p-levels and the continuum states of the two-dimensional layers, heavy and light hole coupling, and elliptic dot confinement potential [23]. We expect in these cases that the emission intensities will depend on the Coulomb interactions. However,

as long as the single particle level spacing is larger than the characteristic Coulomb energy the effect would be minor.

Acknowledgments

This work was supported by grant No. R01-2005-000-10352-0 from the Basic Research Program of the

Korea Science and Engineering Foundation, by Quantum Functional Semiconductor Research Center (QSRC) at Dongguk University of the Korea Science and Engineering Foundation and by Pure Basic Research Group project of Korea Research Foundation under Grant No. C00054. This work was supported by The Second Brain 21 Project.

-
- [1] G. W. Bryant and G.S. Solomon, *Optics of Quantum Dots and Wires*, (Artech House, Norwood, 2005).
 - [2] P. Michler, A. Kiraz, C. Becher, W. V. Schoenfeld, P. M. Petroff, Lidong Zhang, E. Hu and A. Imamoglu, *Science* **290**, 2282 (2000).
 - [3] Z. Yuan, B. E. Kardynal, R. M. Stevenson, A. J. Shields, C. J. Lobo, K. Cooper, N. S. Beattie, D. A. Ritchie and M. Pepper, *Science* **295**, 102 (2002).
 - [4] J.-Y. Marzin, J.-M. Gérard, A. Izraël, D. Barrier, and G. Bastard, *Phys. Rev. Lett.* **73**, 716 (1994).
 - [5] S. Fafard, R. Leon, D. Leonard, J. L. Merz, and P. M. Petroff, *Phys. Rev. B* **52**, 5752 (1995).
 - [6] W. Yang, H. Lee, T.J. Johnson, P.C. Serce, and A. G. Norman, *Phys. Rev. B* **61**, 2784 (2000).
 - [7] E. Dekel, D. Gershoni, E. Ehrenfreund, D. Spektor, J. M. García, and P. M. Petroff, *Phys. Rev. Lett.* **80**, 4991 (1988).
 - [8] E. Dekel, D. Gershoni, E. Ehrenfreund, J. García, and P. M. Petroff, *Phys. Rev. B* **61**, 11009 (2000).
 - [9] L. Landin and M.-E. Pistol, C. Pryor, M. Persson, L. Sammuelsen, and M. Miller, *Phys. Rev. B* **60**, 16640 (1999).
 - [10] Y. Toda, O. Moriwake, M. Nishioda, and Y. Arakawa, *Phys. Rev. Lett.* **82**, 4114 (1999).
 - [11] A. Zrenner, *J. Chem. Phys.* **112**, 7790 (2000).
 - [12] G. W. Bryant, *Phys. Rev. B* **37**, 8763 (1988).
 - [13] G. W. Bryant, *Phys. Rev. B* **41**, 1243 (1990).
 - [14] E. Dekel et al, *Phys. Rev. Lett.* **80**, 4991 (1998).
 - [15] M. Ikezawa, S. V. Nair, H.-W. Ren, Y. Masumoto, and H. Ruda, *Phys. Rev. B* **73**, 125321 (2006).
 - [16] A. Barenco and M.A. Dupertuis, *Phys. Rev. B* **52**, 2766 (1995).
 - [17] P. Hawrylak, *Phys. Rev. B* **60** 5597 (1999).
 - [18] J. Shumway, A. Franceschetti, and A. Zunger, *Phys. Rev. B* **63**, 155316 (2001).
 - [19] S. Corni, M. Brasken, M. Lindberg, and J. Olsen, and D. Sundholm, *Phys. Rev. B* **67**, 085314 (2003).
 - [20] S.-R. Eric Yang, J. Yeo, and S. Han, *Phys. Rev. B* **71**, 245307 (2005).
 - [21] K. Karrai, R. J. Warburton, C. Schulhauser, A. Högele, B. Urbaszek, E. J. McGhee, A. O. Govorov, J. M. Garcia, B. D. Gerardot and P. M. Petroff, *Nature* **427**, 135 (2004).
 - [22] In Ref. [17] the couplings from the p-shell to d-shell and to the continuum states of the two-dimensional layers are ignored. However, if excitations from the s- to p-shells are significant then so are excitations from the p- to d-shells since the probabilities for these excitations have the same order of magnitude. If the barrier height of the quantum dots is small d-shells may not exist. Even in this case excitations from the p-shell to the continuum states of the two-dimensional layers must be included, see Ref. [21].
 - [23] S. Park and S.-R. Eric Yang, *Phys. Rev. B* **72**, 125410 (2005).
-

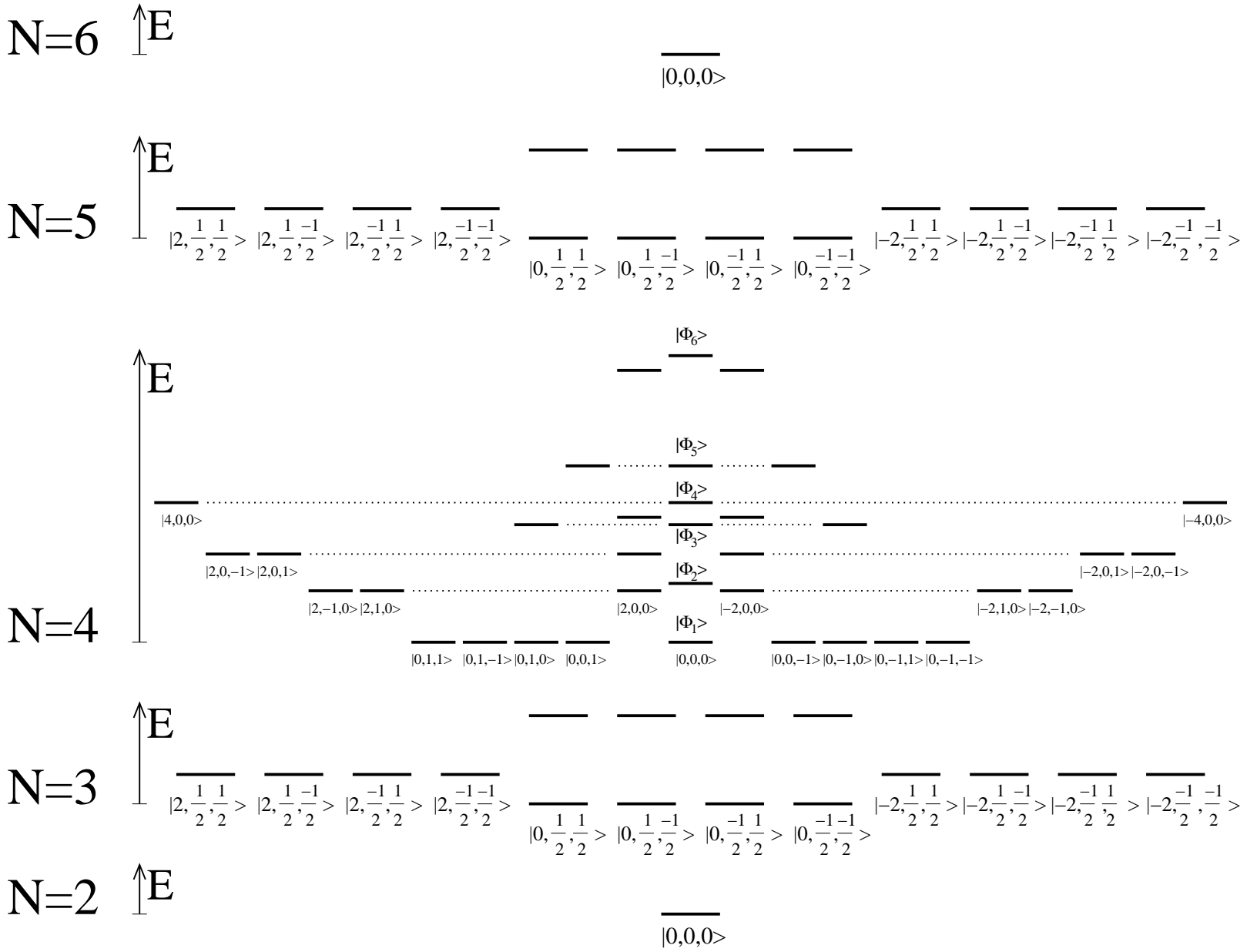


FIG. 5: Energy levels of each Hilbert subspace $|L_z, S_{e,z}, S_{h,z}\rangle$. The dimension of each subspace is equal to the number of energy levels displayed. For $N = 4$ the states in the four dimensional Hilbert subspaces $|2, 0, 0\rangle$, $|-2, 0, 0\rangle$ are optically inactive.